

A simple model for estimating a magnetic field in laser-driven coils

Gennady Fiksel,^{1,a)} William Fox,² Lan Gao,² and Hantao Ji³

¹Center for Ultrafast Optical Science, University of Michigan, Ann Arbor, Michigan 48109, USA

²Princeton Plasma Physics Laboratory, Princeton University, Princeton, New Jersey 08543, USA

³Department of Astrophysical Sciences, Princeton University, Princeton, New Jersey 08544, USA

(Received 16 August 2016; accepted 15 September 2016; published online 28 September 2016)

Magnetic field generation by laser-driven coils is a promising way of magnetizing plasma in laboratory high-energy-density plasma experiments. A typical configuration consists of two electrodes—one electrode is irradiated with a high-intensity laser beam and another electrode collects charged particles from the expanding plasma. The two electrodes are separated by a narrow gap forming a capacitor-like configuration and are connected with a conducting wire-coil. The charge-separation in the expanding plasma builds up a potential difference between the electrodes that drives the electrical current in the coil. A magnetic field of tens to hundreds of Teslas generated inside the coil has been reported. This paper presents a simple model that estimates the magnetic field using simple assumptions. The results are compared with the published experimental data. *Published by AIP Publishing.* [<http://dx.doi.org/10.1063/1.4963763>]

Starting with the pioneering work by Diado *et al.*,¹ several experiments have presented results on a very promising method for generating a magnetic field with a laser-driven coil.^{1–5} A typical experimental setup consists of two metal electrodes connected with a conducting wire-coil. A hot-electron plasma is produced by irradiating one of the electrodes with a high-intensity laser beam while another electrode collects charged particles from the expanding plasma. The charge-separation in the expanding plasma builds up a potential difference between the electrodes that drives the electrical current in the coil.

While some of the experiments cited above bear close similarities in terms of the geometry and the size of the electrodes as well as the laser parameters, the reported values of the magnetic field and especially the efficiency of conversion of the laser energy to the magnetic field energy are drastically different. For example, Gao *et al.*⁵ reported a magnetic field of ~ 40 T and a conversion efficiency of $\sim 0.01\%$, whereas Fujioka *et al.*⁴ reported a magnetic field of ~ 1000 T and a conversion efficiency of $\sim 1500\%$! The latter is not a typo: the estimated magnetic field energy was 15 kJ, while the laser energy was 1 kJ. One reason for the discrepancy could be misinterpretation of the data from the diagnostic methods used for magnetic field measurement. In Refs. 2–4, a B-dot probe that was used for field measurement was placed at a significant distance from the coil—one hundred times the coil radius. Inferring the magnetic field at the coil position carries an extrapolation of six orders of magnitude that could produce a significant error. In Ref. 5, the magnetic field was inferred from the deflection of energetic protons passing directly through the magnetized area, so the measurement errors were minimized.

This paper presents a simple model that calculates the generated magnetic field using very basic assumptions and compares the results with published experimental data.

Consider an experimental setup shown in Fig. 1. A laser beam ablates plasma from the target electrode, and the

plasma expands toward the front electrode. During the expansion, the hot plasma electrons stream ahead of the heavier ions, and as a result, the front plate, which collects the charged plasma particles, charges negatively. This negative voltage drives electric current through the coil connecting the front and the back electrodes.

A simple model for collisionless plasma expansion into vacuum was introduced by Mora.⁶ In that model, the plasma density forms a spatial profile that depends on the time, t , and the distance from the target, x , as

$$n_e = n_{e0} \exp(-x/c_s t), \quad (1)$$

where n_{e0} is the initial electron density, $c_s = (ZT_e/Am_p)^{1/2}$ is the ion sound speed, and T_e (expressed hereafter in electron-volts) is the electron temperature. The corresponding space-charge electric field is

$$E = T_e/c_s t. \quad (2)$$

In zeroth order, one can derive the potential difference between the electrodes from Eq. (2) and use it to determine the coil current I_c via Ohm's law

$$-U = \int_0^d E dx = T_e d/c_s t = RI_c + L \frac{dI_c}{dt}, \quad (3)$$

where d is the distance between the electrodes, and L and R are the coil inductance and resistance, respectively.

We will expand this model to account for (a) the rate of charged particle generation, (b) the effects of charging of the capacitor formed by the electrodes, and (c) non-Maxwellian features of the electron distribution function. In particular, accounting for the ablation rate appears to be necessary, at least in principle. Indeed, because the charged particle generation is not accounted for in Eq. (3), then it might appear that even a very few plasma electrons, even if they are very energetic, can drive a large current through the coil, which is unphysical. Second, the charging of the front electrode creates a potential barrier for the electrons

^{a)}gfiksel@umich.edu

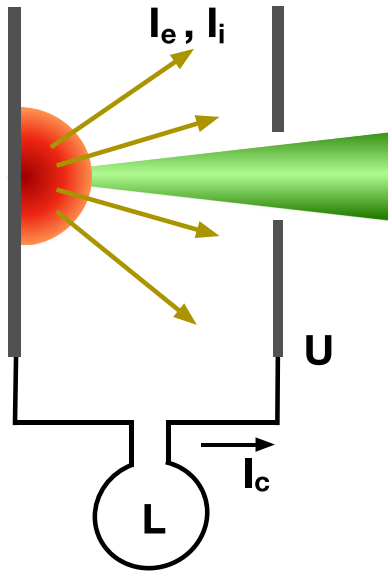


FIG. 1. A typical experimental setup consists of two electrodes connected with a wire-coil. A hot-electron plasma is produced by irradiating one of the electrodes with a high-intensity laser beam. The charge-separation in the expanding plasma electrons (I_e) and ions (I_i) builds up a potential difference U between the electrodes that drives electrical current I_c through the coil L .

affecting the dynamics of plasma expansion—a feature absent from Mora’s model.

According to the ablation model by Atzeni,⁷ the electron generation rate can be approximated by $\dot{N}_e = n_c c_T A_L$, where $n_c = 1.1 \times 10^{27} / \lambda_L^2 \text{ m}^{-3}$ is the critical density, λ_L is the laser wavelength in μm , and A_L is the area of the laser ablation spot. The ablation velocity c_T is very close to the ion acoustic speed $c_s = (ZT_e / Am_p)^{1/2}$, whereas the electron temperature T_e depends on the laser intensity and the regime of laser absorption. If the intensity $I_L \lambda^2$ exceeds $10^{16} \text{ W/cm}^2 \mu\text{m}^2$, the temperature can be over 10 keV.²

Consider a typical example of a laser beam with $\lambda = 0.35 \mu\text{m}$ and $A_L = 0.01 \text{ mm}^2$ ablating a plasma with $T_e = 10 \text{ keV}$ and $Z/A = 0.5$. These parameters, $n_c = 9 \times 10^{27} \text{ m}^{-3}$, $c_s = 7 \times 10^5 \text{ m/s}$ result in $\dot{N}_e = 6.3 \times 10^{25} \text{ s}^{-1}$, which corresponds to the charged particle current of $I_0 = e\dot{N}_e = 11 \text{ MA}$. Naturally, this current (equal in magnitude but opposite in sign for ions and electrons) represents an absolute limit of the current that can be driven in an external circuit.

Consider a gap with the electrodes not connected to each other. The gap charging is governed by the difference between the ion and electron currents through the gap

$$\frac{dQ}{dt} = C \frac{dU}{dt} = I_i - I_e, \quad (4)$$

where C is the gap capacitance.

Assume the following (heuristic) model for the ion and electron currents: $I_i = I_0 \exp(-d/c_s t)$ and $I_e = I_0 \exp(U/T_e)$. The exponential term in the ion current mimics Mora’s plasma expansion with the finite speed of propagation of the ion component through the gap of a thickness d . The exponential factor in the electron term reflects the repelling of Maxwellian electrons with a temperature T_e by the front electrode negative potential U . With that, Eq. (4) can be written as

$$\frac{dQ}{dt} = C \frac{dU}{dt} = I_i - I_e = I_0 e^{-d/c_s t} - I_0 e^{U/T_e}. \quad (5)$$

Admittedly, Eq. (5) is not quite accurate, especially during the initial stage of plasma expansion because it does not account for the space charge effects and plasma quasineutrality. Also, Eq. (5) presumes a very large electron current flowing through the gap at the initial moment. We also neglect the fact that some electrons can escape the capacitor either through the hole in the front electrode or through the open sides, so the assumed electron current is certainly an overestimation of its actual value. Nevertheless, it constitutes the upper-bound estimate of the number of electrons participating in the electric current creation and, as such, yields an upper-bound estimate of the load current and thus the magnetic field.

In addition, the characteristic capacitor charging time is very short— $\tau_c \sim CT_e/I_0 = 10^{-16} \text{ s}$ for $C = 0.1 \text{ pF}$, $T_e = 10 \text{ keV}$, and $I_0 = 10 \text{ MA}$. Therefore, the gap front electrode is charged very quickly to a voltage required to equalize the ion and electron currents $-U = T_e d/c_s t$, which is equivalent to that obtained from Mora’s expansion model, specifically Eq. (3).

The waveform of the potential derived from Eq. (5) for the above plasma parameters and $d = 1 \text{ mm}$ and $C = 0.1 \text{ pF}$ is shown in Fig. 2 (blue line). The gap charges quickly to $\sim 10 \times T_e$ and then falls on the ion transit time scale. The model avoids the divergence in Mora’s solution (Eq. (3), shown in red line) by incorporating the charging of the capacitor. The capacitor in question can be physical, formed by the electrodes, or even virtual, formed by the gap between the expanding quasi-neutral plasma and the front electrode. After a short charging period, the two solutions agree well for $t c_s/d \geq 0.1$. Incidentally, it corresponds to the time $t > t_M$ when the quasi-neutrality approach by Mora’s model becomes valid over the whole space between the electrodes. Here, t_M is the time when the ion front of the expanding plasma has reached the front electrode and is determined from⁶

$$t_M = \frac{d}{c_s} \left[2 \ln \left(\frac{d}{\lambda_D} \frac{t_M c_s}{d} \right) + \ln 2 - 3 \right]^{-1}, \quad (6)$$

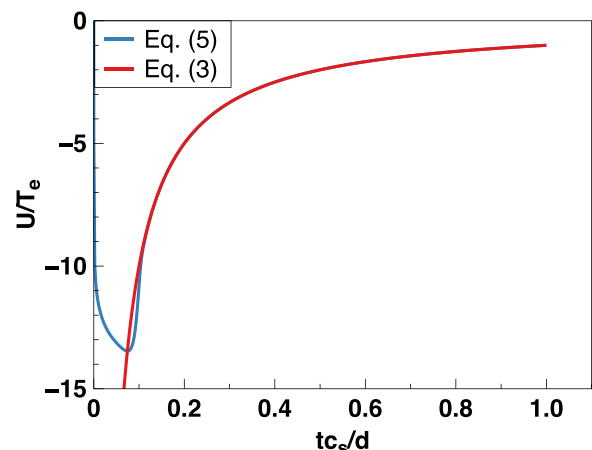


FIG. 2. Voltage waveform for an isolated gap. Blue line—solution of Eq. (5). Red line—solution of Eq. (3). The voltage is measured in units of T_e and the time is measured in units of d/c_s .

which results in $t_{Mc_s}/d \approx 0.07$ for the above conditions. The Debye radius λ_D is calculated for the ablation density n_c and plasma temperature T_e .

Consider an experimental setup described in Ref. 5. The experiment was conducted at the OMEGA EP Laser System⁸ of the Laboratory for Laser Energetics of the University of Rochester, New York. The back electrode is irradiated with two laser beams with a total energy of $E_L = 2.5$ kJ and focused to a $100 \mu\text{m}$ -diameter spot to an intensity of $I_L = 3 \times 10^{16}$ W/cm². The laser wavelength is $\lambda = 0.35 \mu\text{m}$. The gap electrodes, separated by $d = 0.6$ mm, are connected with a single wire loop with a radius of $a = 0.3$ mm, an inductance of $L = 1.2$ nH, and a resistance of $R = 0.1 \Omega$. The magnetic field in the vicinity of the wire was measured by the proton deflectometry diagnostic.

The gap charging drives a current I_c through the coil, so Eq. (5) is now modified by the addition of the coil current

$$C \frac{dU}{dt} = I_0 e^{-d/c_s t} - I_0 e^{U/T_c} + I_c, \quad (7)$$

while the coil current drive I_c is described by

$$-U = RI_c + L \frac{dI_c}{dt}. \quad (8)$$

The waveform of the coil current under an assumption of Maxwellian electrons with $T_e = 10$ keV is shown in Fig. 3 (red line). The model result is very close to the experimental data of $I_c = 22$ kA at $t = 3.1$ ns. The magnetic field amplitude calculated at the coil center under the same assumptions is $B = 42$ T, in agreement with the experimental data of $B = 40 - 50$ T at $t = 3.1$ ns. The maximum magnetic field energy is $E_B = 0.25$ J, which is about 0.01% of the laser energy.

Depending on a specific regime of laser energy absorption, the plasma electron distribution can be different from single Maxwellian. At high laser intensity, the laser beam can be absorbed through the resonance absorption and generate a high-energy electron tail. Assume that of all the ablated electrons, a fraction K_h is hot with a temperature T_h , whereas the bulk fraction $(1 - K_h)$ is cold with a temperature T_c .

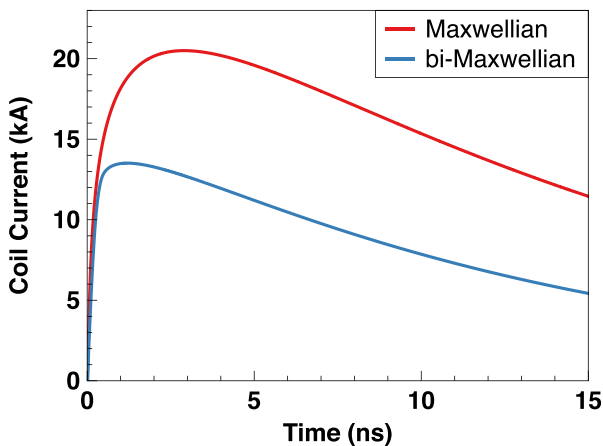


FIG. 3. Red line—coil current for an experimental setup described in Ref. 5. The electrons are presumed Maxwellian with a temperature $T_e = 10$ keV. Blue line—the electrons are presumed bi-Maxwellian, comprised of 10% of $T_e = 10$ keV electrons and 90% of $T_e = 1$ keV electrons.

Then, the gap charging Eq. (7) can be modified to include two groups of electrons

$$C \frac{dU}{dt} = I_0 e^{-d/c_s t} - (1 - K_h) e^{U/T_c} - K_h e^{U/T_h} + I_c, \quad (9)$$

while the coil current drive I_c is still described by Eq. (8). The ion acoustic speed in Eq. (9) is $c_s = (ZT_{eff}/Am_p)^{1/2}$, where T_{eff} is an “effective” temperature that we define as $T_{eff} = (n_{ec}T_c + n_{eh}T_h)/n_e$. Calculating the moments of the electron distribution function yields

$$T_{eff} = T_h \frac{K_h + (1 - K_h) \sqrt{T_c/T_h}}{K_h + (1 - K_h) \sqrt{T_h/T_c}}. \quad (10)$$

The waveform of the coil current for $T_h = 10$ keV, $T_c = 1$ keV, and the fraction of hot electrons $K_h = 0.1$ is shown as a blue line in Fig. 3. Even though the fraction of hot electrons is lowered by a factor of 10, the current is reduced by only a factor of 1.5. This example illustrates the dominant role of the fast electrons in current generation.

This paper presents a simple model of a laser-generated magnetic field accounting for (a) the rate of charged particle generation, (b) the effects of charging of the capacitor formed by the electrodes, and (c) non-Maxwellian features of the electron distribution function. The results of the modeling of the experimental setup described in Ref. 5 are very close to the experimental data.

The model also allows to assess critically the claims of super-high kilo-tesla magnetic fields.^{4,9,10} Indeed, consider, for example, a setup described in Ref. 9. The back electrode is irradiated with a laser beam with an energy of $E_L = 500$ J, a wavelength of $\lambda = 1.057 \mu\text{m}$, a duration of $\tau_L = 1$ ns, and an intensity of $I_L = 10^{17}$ W/cm². The gap electrodes, separated by $d = 0.9$ mm, are connected with a single wire loop with a radius of $a = 0.25$ mm, an inductance of $L \sim 2$ nH (including the leads), and a room-temperature resistance of $R \sim 0.03 \Omega$. The proton radiography results indicated $B \sim 100$ T at the coil center. To produce such a field, requires, according to our model, a plasma with an electron temperature of roughly 40 keV, which is quite possible at such a high laser intensity. However, to produce an 800 T field would require a temperature in excess of 500 keV, which seems to be unrealistic.

Another issue, although not directly related to the subject of this paper, is the resistive heating of the coil wire. For the large current of ~ 300 kA required to create the high field,^{9,10} the resistive heat dissipated in the wire is about 1.5 J. For the wire volume of $\sim 5 \times 10^{-3}$ mm³, the wire would be heated to about 10^5 °K, which means the wire would be evaporated long before the end of the laser pulse. The heating estimate would be even higher, taking into account the resistivity dependence on the temperature and the skin effect (the skin layer is only about $10 \mu\text{m}$ on the time scale of 1 ns).

The experimental results from the OMEGA EP Laser System of the Laboratory for Laser Energetics were obtained while supported by the National Laser Users Facility Grant No. DE-NA0002205.

- ¹H. Daido, F. Miki, K. Mima, M. Fujita, K. Sawai, H. Fujita, Y. Kitagawa, S. Nakai, and C. Yamanaka, *Phys. Rev. Lett.* **56**, 846 (1986).
- ²C. Courtois, A. D. Ash, D. M. Chambers, R. Grundy, and N. C. Woolsey, *J. Appl. Phys.* **98**, 054913 (2005).
- ³S. Fujioka, Z. Zhang, N. Yamamoto, S. Ohira, Y. Fujii, K. Ishihara, T. Johzaki, A. Sunahara, Y. Arikawa, K. Shigemori, Y. Hironaka, Y. Sakawa, Y. Nakata, J. Kawanaka, H. Nagatomo, H. Shiraga, N. Miyanaga, T. Norimatsu, H. Nishimura, and H. Azechi, *Plasma Phys. Controlled Fusion* **54**, 124042 (2012).
- ⁴S. Fujioka, Z. Zhang, K. Ishihara, K. Shigemori, Y. Hironaka, T. Johzaki, A. Sunahara, N. Yamamoto, H. Nakashima, T. Watanabe, H. Shiraga, H. Nishimura, and H. Azechi, *Nat. Sci. Rep.* **3**, 1170 (2013).
- ⁵L. Gao, H. Ji, G. Fiksel, W. Fox, M. Evans, and N. Alfonso, *Phys. Plasmas* **23**, 043106 (2016).
- ⁶P. Mora, *Phys. Rev. Lett.* **90**, 185002 (2003).
- ⁷S. Atzeni and J. Meyer-Ter-Vehn, *The Physics of Inertial Fusion* (Oxford University Press, 2004).
- ⁸L. J. Waxer, D. N. Maywar, T. J. Kessler, B. E. Kruschwitz, S. J. Loucks, R. L. McCrory, D. D. Meyerhofer, S. F. B. Morse, C. Stoeckl, and J. D. Zuegel, *Opt. Photonics News* **16**, 30 (2005).
- ⁹J. J. Santos, M. Bailly-Grandvaux, L. Giuffrida, P. Forestier-Colleoni, S. Fujioka, Z. Zhang, P. Korneev, R. Bouillaud, S. Dorard, D. Batani, M. Chevrot, J. E. Cross, R. Crowston, J. L. Dubois, J. Gazave, G. Gregori, E. D'Humières, S. Hulin, K. Ishihara, S. Kojima, E. Loyez, J. R. Marquès, A. Morace, P. Nicolai, O. Peyrusse, A. Poyé, D. Raffestin, J. Ribolzi, M. Roth, G. Schaumann, F. Serres, V. T. Tikhonchuk, P. Vacar, and N. Woolsey, *New J. Phys.* **17**, 083051 (2015).
- ¹⁰K. F. F. Law, M. Bailly-Grandvaux, A. Morace, S. Sakata, K. Matsuo, S. Kojima, S. Lee, X. Vaisseau, Y. Arikawa, A. Yogo, K. Kondo, Z. Zhang, C. Bellei, J. J. Santos, S. Fujioka, and H. Azechi, *Appl. Phys. Lett.* **108**, 091104 (2016).